GAP-FILLING BASED ON EOF ANALYSIS OF SPATIO-TEMPORAL COVARIANCE OF SATELLITE IMAGE DERIVED DISPLACEMENT TIME SERIES

A. Hippert-Ferrer, Student Member IEEE*, Y. Yan,* Member IEEE*, P. Bolon,* Member IEEE

LISTIC, Université Savoie Mont-Blanc, Annecy, France

ABSTRACT

An iterative method, namely extended EM-EOF (Expectation Maximization - Empirical Orthogonal Functions) is proposed to retrieve missing values in satellite derived displacement time series. The method constructs the spatio-temporal covariance of a displacement time series, decomposes it into different EOF modes by solving the eigenvalue problem and then selects an optimal number of EOF modes to reconstruct the time series based on cross validation errors. The latter are also used as convergence criterion in an EM-like algorithm. A confidence index associated with each eigenvalue, estimated from the eigenvalue uncertainty, is introduced as a metric for refining the estimated optimal number of EOF modes. Results on simulated displacement time series perturbed by spatially correlated noise demonstrate the potential of extended EM-EOF to impute spatio-temporal missing values even in case of a reduced size of time series.

Index Terms— Gap filling, EOFs, spatio-temporal covariance, satellite image, displacement, time series

1. INTRODUCTION

Time series analysis constitutes a living subject in satellite image derived displacement measurement, especially since the launching of Sentinel satellites that provide free and systematic satellite image acquisitions with reduced revisiting time and extended spatial coverage. Large volumes of satellite images are available for monitoring of numerous targets at the Earth's surface, which allows for significant improvements of the displacement measurement accuracy, benefiting from advanced multi-temporal methods [1, 2]. Regardless of this large volume of data, time series of displacement measurement derived from satellite images can suffer from missing data in both space and time dimensions, mainly due to technical limitations of the ground displacement computation methods (e.g. differential interferometry (InSAR), offset tracking) and surface property changes of the targets under observation [3]. Missing data can hinder or even bias the full understanding of the phenomenon. An efficient missing data reconstruction method is thus of particular importance for all research and applications that require data completeness.

On the other hand, missing data problem in satellite image derived displacement measurement has not yet been paid significant attention. Existing methods are still mainly focused on spatial or temporal interpolation only, which prevents from using the full spatio-temporal information [4]. In [5, 3], authors proposed a namely Expectation Maximization-Empirical Orthogonal Functions (EM-EOF) method based on EOF analysis of the temporal covariance of a displacement time series for missing data reconstruction. Interesting results were obtained in Sentinel-1 InSAR displacement measurement time series, which confirms the efficiency of the EOF analysis for missing data reconstruction. However, the EM-EOF method presents some limitations when 1) the time series is small in size, for example, in alpine glacier displacement measurement by InSAR (InSAR works only in winter without snow cover), 2) the spatial correlation prevails over the temporal correlation and 3) heterogeneous and local spatial features are present in the displacement field.

Therefore, we introduce in this paper an extension to the EM-EOF method, namely extended EM-EOF hereafter, which also makes the use of spatial correlation by augmenting the data with space-lagged information. The optimal number of EOF modes is then determined by the joint use of cross-validation errors and eigenvalues uncertainties. Synthetic simulations are then performed in order to highlight the efficiency of the extended EM-EOF method for reconstructing a displacement time series with the presence of correlated data gaps, significant spatially correlated noise and complex displacement behaviors.

2. METHODOLOGY

Starting from an appropriate initialization of missing values, the extended EM-EOF method is based on an EM-like algorithm. At E step, missing data are updated and the spatio-temporal covariance is estimated and decomposed into EOF modes. At M step, the data are reconstructed with an optimal number of EOF modes that minimizes the difference between the initial and reconstructed data. The reconstructions are then used as initial values of missing data points for the next iteration. The final reconstruction is obtained after the convergence of the iterative process.

2.1. Data organization and covariance estimation

Let $\mathbf{X}$ be a time series (i.e. spatio-temporal data matrix) containing N temporal observations over P spatial samples, which in matrix form can be represented as follows:

$$\mathbf{X} = (\mathbf{x}_1, \mathbf{x}_2, \ldots, \mathbf{x}_N) \tag{1}$$

where each $\mathbf{x}_t$ is a spatial map (e.g. ensemble of pixels of an image) of size $W \times H = P$ at times $t = 1, \ldots, N$. Note that in practice, $\mathbf{X}$ is detrended, i.e. its spatial mean is removed. From $\mathbf{X}$, a "space-lagged" matrix $\mathbf{D}$ can be formed by applying a sliding window of $M \leq P$ spatial samples to each temporal observation $\mathbf{x}_t$ (Fig. 1). $\mathbf{D}$ is called the augmented data matrix (as in [6]) of size $K \times MN$ with $K = (W - \sqrt{M} + 1)(H - \sqrt{M} + 1)$:

$$\mathbf{D} = (\mathbf{d}_1, \mathbf{d}_2, \ldots, \mathbf{d}_K)^T \tag{2}$$

where $\mathbf{d}_i$ is an MN-length vector.

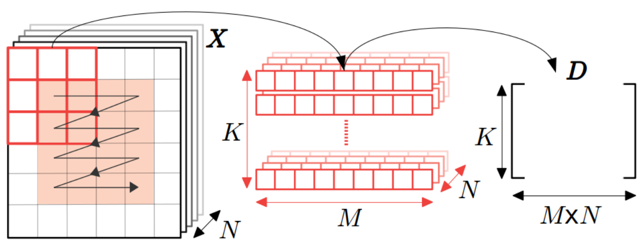

Fig. 1: Illustration of the augmentation of data matrix $\mathbf{X}$ with $M = 9$ and $K = 16$. A M-samples spatial squared window (in red) is applied to each $\mathbf{x}_t$ and slides through K possible positions. Each view of the M-samples window is then vectorized and put into a $K \times M \times N$ intermediary matrix. Finally, dimension $M \times N$ is vectorized to get matrix $\mathbf{D}$.

The spatio-temporal covariance $\mathbf{C}$ of the augmented data matrix $\mathbf{D}$ can be then estimated as:

$$\hat{\mathbf{C}} = \frac{1}{K-1}\mathbf{D}^T\mathbf{D} \tag{3}$$

2.2. Spatio-temporal covariance decomposition

The eigenvalue decomposition of matrix $\hat{\mathbf{C}}$ yields to:

$$\hat{\mathbf{C}} \overset{EVD}{=} \sum_{i=1}^{MN} \lambda_i \mathbf{u}_i \mathbf{u}_i^T \tag{4}$$

where $\mathbf{u}_i$ is an eigenvector of $\hat{\mathbf{C}}$ corresponding to the eigenvalue λ_i. Each term $\lambda_i \mathbf{u}_i \mathbf{u}_i^T$ corresponds to an EOF mode which describes the spatio-temporal variability of the augmented data matrix $\mathbf{D}$.

2.3. Reconstruction of the data matrix

From equation (4), the augmented matrix $\mathbf{D}$ can be reconstructed in the following way:

$$\hat{\mathbf{D}} = \sum_{i=1}^{MN} \mathbf{D}\mathbf{u}_i \mathbf{u}_i^T \tag{5}$$

where $\mathbf{D}\mathbf{u}_i = \mathbf{a}_i$ are the principal components (PCs) of $\mathbf{D}$. Each $\mathbf{x}_i$ can then be retrieved from $\hat{\mathbf{D}}$ by reversing the formatting described above (Section 2.1, Fig. 1). Since the first EOF modes explain most the variance of the data matrix and higher order EOF modes often correspond to noise, the truncation of (5) by a number $R \ll MN$ of PCs and EOFs allows mainly to preserve the displacement signal.

2.4. Selection of the optimal number of EOF modes

To determine the optimal R which best reconstructs the displacement signal, the first metric used is the cross-validation root-mean-square error (cross-RMSE) defined as the ℓ_2-norm of the difference between the cross-validation data and the reconstruction [5]. The optimal number of EOFs modes is then found as the one that minimizes the cross-RMSE. However, with this metric, strong mixing between the correlated noise and the displacement signal can lead to an over-estimation of R, which can be explained by the fact that cross-validation data are also subject to noise [3, 7]. To overcome this issue, we propose to make use of the degeneracy (close eigenvalues) and/or the separation (distant eigenvalues) in the eigenvalues spectrum, which provides useful information on the frequencies distributions and the spatio-temporal variability of the signal. Two or multiple consecutive eigenvalues (called multiplet) are degenerate when the uncertainty of an eigenvalue λ_k is comparable with or larger than the spacing between λ_k and its closest neighbor. Therefore, to investigate multiplet degeneracy, eigenvalues uncertainties must be first estimated. [8] proposed a "rule of thumb" to approximate the eigenvalues uncertainties:

$$\Delta\lambda_k \approx \sqrt{\frac{2}{M^*N^*}}\lambda_k \qquad \Delta\mathbf{u}_k \approx \frac{\Delta\lambda_k}{\lambda_j - \lambda_k}\mathbf{u}_j \tag{6}$$

where λ_j is the closest eigenvalue from λ_k, $\mathbf{u}_j$ and $\mathbf{u}_k$ are the corresponding eigenvectors, M^*N^* is the number of independent observations in the spatio-temporal sample, also called effective sample size. The interpretation of equation (6) is the following: if the uncertainty of eigenvalue λ_k is close to the difference between λ_k and λ_j, then the corresponding eigenvectors, $\mathbf{u}_j$ and $\mathbf{u}_k$, are likely to be contaminated each other. According to [9], the estimation of N^* is given by:

$$N^* = N\big[1 + 2\sum_{k=1}^{N-1}(1 - \frac{k}{N})\rho(k)\big]^{-1} \tag{7}$$

where $\rho(k)$ is the temporal auto-correlation of the time series and N is the number of observations in time. This definition holds for a univariate time series of N observations, e.g. a pixel value varying over time. Following this definition, we estimate the effective sample size M^* within each spatial window of size M used to augment the data matrix $\mathbf{X}$:

$$M^* = M\left(1 + \frac{2}{N}\sum_{k=1}^{M}(1 - \frac{k}{M})\sum_{t=1}^{N} I_t\right)^{-1} \quad (8)$$

where I_s is the Moran's I statistics [10] for estimating spatial auto-correlation of the spatial map at time t.

Based on the estimated eigenvalues uncertainties given in equation (6), a second metric consisting of a confidence measure, $\mathcal{C}_k$, associated with each eigenvalue λ_k can be computed in the $[0, 1]$ interval:

$$\mathcal{C}_k = \frac{\max(\Gamma_k) - \Gamma_k}{\max(\Gamma_k) - \min(\Gamma_k)} \quad (9)$$

with $\Gamma_k = \log\left(\frac{\Delta\lambda_k}{\lambda_j - \lambda_k}\right)$, $k = 1, \dots, nM$. $\mathcal{C}_k$ allows detecting the degeneracy or the separation of the eigenvalues in the spectrum, which respectively corresponds to lower and higher values of $\mathcal{C}_k$. That is, any peak in $\mathcal{C}_k$ will coincide with a separation between two eigenvalue multiplets, whereas lower "sidepeak" values correspond to the degeneracy of a multiplet. To refine the optimal number of EOF modes R primarily determined using the cross-RMSE, $\mathcal{C}_k$ is computed for $k = 1, \dots, MN$. Then, the peaks in $\mathcal{C}_k$ corresponding to the separations in the eigenvalue spectrum are detected. If one peak has an index k corresponding to R, the algorithm stops here. Otherwise, if the index is different from R and if $\mathcal{C}_k$ is high enough (e.g. $\mathcal{C}_k \geq 0.6$), the optimal number is updated so that it matches the index k.

2.5. Determination of the lag M

In general, the choice of M is dictated by a trade-off between the amount of information extracted in the window (M should be large) and the number of repetitions of the window within each image (M should be small) [11]. Instead of a single value, a range of M can provide satisfactory results. In this paper, two metrics are proposed to determine the range of M. The first metric is based on the covariance estimation theory, that is, the number of independent samples should be at least twice the number of variables. Thus, the maximum value of M can be determined by solving $K > 2M$, which leads approximately to $M < P/6$. The second metric is based on the spatial auto-correlation property of the displacement field. Let τ the spatial decorrelation decay defined as:

$$\tau = -\frac{\Delta P}{\log r} \quad (10)$$

where r is the lag-one auto-correlation and ΔP is the spatial sampling rate, here 1 pixel. Following [6], M can be approximated by $M \simeq P/\tau$. In most cases, r is supposed to be smaller than 0.95, thus $M > P/20$.

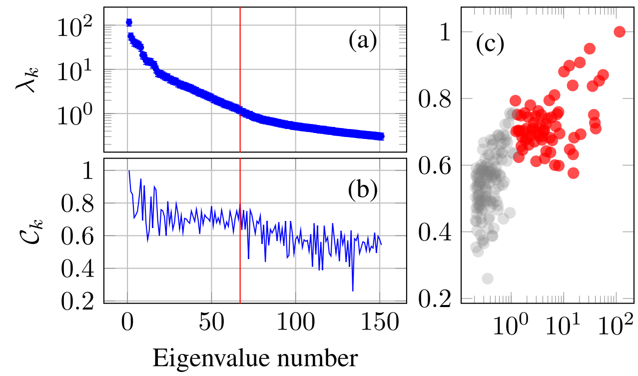

Fig. 2: a) Eigenvalues λ_k (first 150 shown) of matrix D, b) associated confidence index $\mathcal{C}_k$ and c) plot of $\mathcal{C}_k$ vs. λ_k showing the eigenvalues corresponding to the number of selected EOF modes (red dots), which corresponds to a peak in $\mathcal{C}_k$ (red vertical line).

3. SYNTHETIC SIMULATIONS

A time series of 10 displacement fields of size 50×50 is generated (relatively small spatial dimension mainly due to computational time). The displacement signal represents oscillations with different frequencies following the model:

$$\begin{aligned} g(r,t) &= \sin(w_1 t)\cos(w_1 r) + 0.5\cos(w_2 t)\cos(w_3 r) \\ &\quad + 0.1\sin(w_4 t)\cos(w_5 r) + 0.3\sin(w_6 r)\sin(w_7 t) \\ &\quad + 0.1\sin(w_8 r)\sin(w_8 t) \end{aligned}$$

for $t = 1, \dots, 10$ and $r_{x,y} = \exp(-(x+y)^2) + \tan(x)$ with (x, y) varying regularly in the $[-1, 1]^2$ grid. Finally, $w_i = 2\pi f_i$ with $f_i = \{0.25, 0.75, 2.5, 1.25, 5, 7.5, 1.75, 0.5\}$.

The displacement signal is then perturbed by spatially correlated noise and spatio-temporally correlated gaps. These features are consistent with observations in real displacement time series obtained from SAR images. Noise and gaps are generated as in [3]. Besides the complexity of the displacement behavior, a relatively low signal-to-noise ratio (SNR), 1.3, and a large gap quantity, 50%, are chosen to confront the extended EM-EOF to a challenging case. The lag was fixed to $M = 121$, which corresponds to the theoretical lower bound of M given $P = 2500$. In this experiment, the estimated optimal number of EOF modes, R, is 67. Figure 2 shows that R corresponds to a peak in $\mathcal{C}_k$, which keeps most of the significant multiplets in the reconstruction, thus preserving the structure of the corresponding EOFs. Note that the level of confidence can be adjusted such that only the peaks situated above a given value are considered.

Figure 3 shows an example of the reconstructed field by extended EM-EOF and the comparison with EM-EOF. A global agreement of displacement pattern between the reconstructed and true fields is observed, given the low SNR, large data gaps, small time series size and complex displacement behaviors. Compared to EM-EOF, the reconstructed field

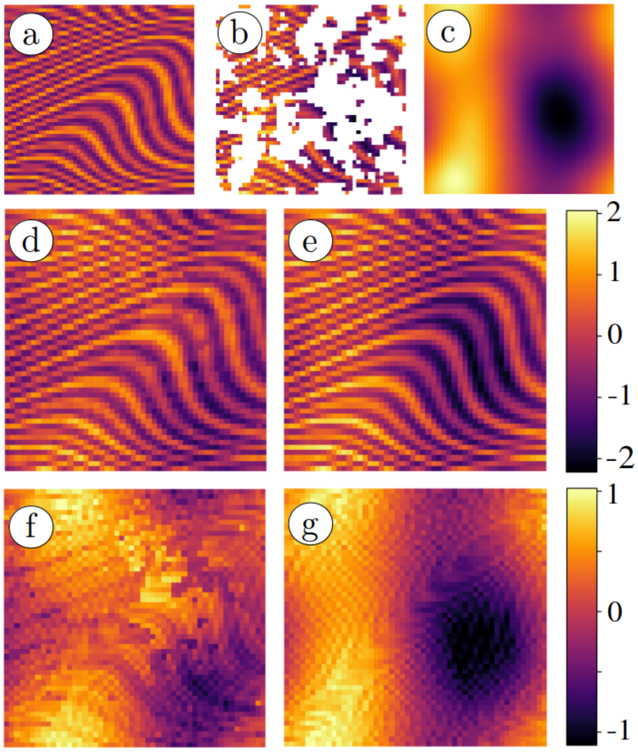

Fig. 3: a) True displacement field $g(r,t)$ at $t = 10$ b) noisy and gappy (50%) displacement field c) spatially correlated noise, d) and e) reconstructed displacement fields with EM-EOF and extended EM-EOF respectively f) and g) residuals (difference between a) and d) or e)).

with extended EM-EOF shows a better result: pattern edges are better preserved and residuals are similar to noise, which is mainly due to the inclusion of space-lagged information, allowing 1) taking advantage of the spatial correlation in addition to the temporal correlation 2) processing spatial samples by small windows with more homogeneous samples.

4. CONCLUSIONS

In this paper, a data adaptive method based on EOF analysis, called extended EM-EOF, is proposed to reconstruct missing data in displacement time series obtained from satellite images. This method explores the spatio-temporal covariance matrix of a time series and proposes robust metrics for the determination of the optimal number of EOF modes for reconstruction. Synthetic simulations with large data gaps and low SNR suggest that this method is particularly efficient in case of heterogeneous local features and small time series size where it can provide a better representation of displacement patterns than the EM-EOF method. In addition, the proposed confidence index associated with eigenvalue uncertainties is of particular interest to enhance the selection of the optimal number of EOFs modes and to prevent from overfitting [4, 5, 7] in case of multiplet degeneracy. The extended EM-EOF method will be applied to offset tracking displacement time series over the Fox glacier in Southern Alps of New Zealand.

Acknowledgment

This work has been supported by the Programme National de Télédétection Spatiale (PNTS, http://www.insu.cnrs.fr/pnts), grant PNTS-2019-11, and by the SIRGA projet funded by Université Savoie Mont Blanc.

5. REFERENCES

[1] Y. Yan, A. Dehecq, E. Trouve, G. Mauris, N. Gourmelen, and F. Vernier, "Fusion of remotely sensed displacement measurements: Current status and challenges," *IEEE Geosci. Remote Sens. Mag.*, vol. 4, no. 1, pp. 6–25, March 2016.

[2] Rémi Prébet, Yajing Yan, Matthias Jauvin, and Emmanuel Trouvé, "A data-adaptative eof based method for displacement signal retrieval from insar displacement measurement time series for decorrelating targets," *IEEE Trans. Geosci. Remote Sens.*, vol. 57, no. 8, pp. 5829–5852, 2019.

[3] Alexandre Hippert-Ferrer, Yajing Yan, and Philippe Bolon, "EM-EOF: gap-filling in incomplete SAR displacement time series," *IEEE Trans. Geosci. Remote Sens.*, under review.

[4] Guojie Wang, Damien Garcia, Yi Liu, Richard de Jeu, and A. Johannes Dolman, "A three-dimensional gap filling method for large geophysical datasets: Application to global satellite soil moisture observations," *Environ. Modelling & Software*, vol. 30, pp. 139 – 142, 2012.

[5] Alexandre Hippert-Ferrer, Yajing Yan, and Philippe Bolon, "Gap-filling based on iterative EOF analysis of temporal covariance : application to InSAR displacement time series," in *IGARSS*, 2019, pp. 262–265.

[6] M. Ghil, M.R. Allen, M. D Dettinger, K. Ide, D. Kondrashov, M.E. Mann, A.W. Robertson, A. Saunders, Y. Tian, F. Varadi, and P. Yiou, "Advanced spectral methods for climatic time series.," *Review of Geophysics*, vol. 40, 1, pp. 1–41, 2002.

[7] Andrew Y. Ng, "Preventing "overfitting" of cross-validation data," in *ICML*, 1997, p. 245–253.

[8] Gerald R. North, Thomas L. Bell, Robert F. Cahalan, and Fanthune J. Moeng, "Sampling errors in the estimation of empirical orthogonal functions," *Monthly Weather Review*, vol. 110, no. 7, pp. 699–706, 1982.

[9] H. J. Thiébaux and F. W. Zwiers, "The interpretation and estimation of effective sample size," *J. Climate Appl. Meteor.*, vol. 23, no. 5, pp. 800–811, 1984.

[10] A.D. Cliff and J.K. Ord, *Spatial Processes: Models and Applications*, Pion, London, 1981.

[11] Andreas Groth and Michael Ghil, "Monte carlo singular spectrum analysis (SSA) revisited: Detecting oscillator clusters in multivariate datasets," *J. Climate*, vol. 28, no. 19, pp. 7873–7893, 2015.